

## Supplementary Materials

### **A promising Ruddlesden-Popper oxide cathode for both proton-conducting and oxygen ionic-conducting solid oxide fuel cells**

Shujun Peng <sup>a</sup>, Song Lei <sup>b</sup>, Sisi Wen <sup>b</sup>, Xingyao Liu <sup>b</sup> and Jian Xue <sup>b, \*</sup>

*a School of Chemistry & Chemical Engineering, Jinggangshan University, Ji'an 343009, China*

*b School of Chemistry & Chemical Engineering, Guangdong Provincial Key Lab of Green Chemical Product Technology, South China University of Technology, No. 381 Wushan Road, Guangzhou 510640, China, Email: xuejian@scut.edu.cn*

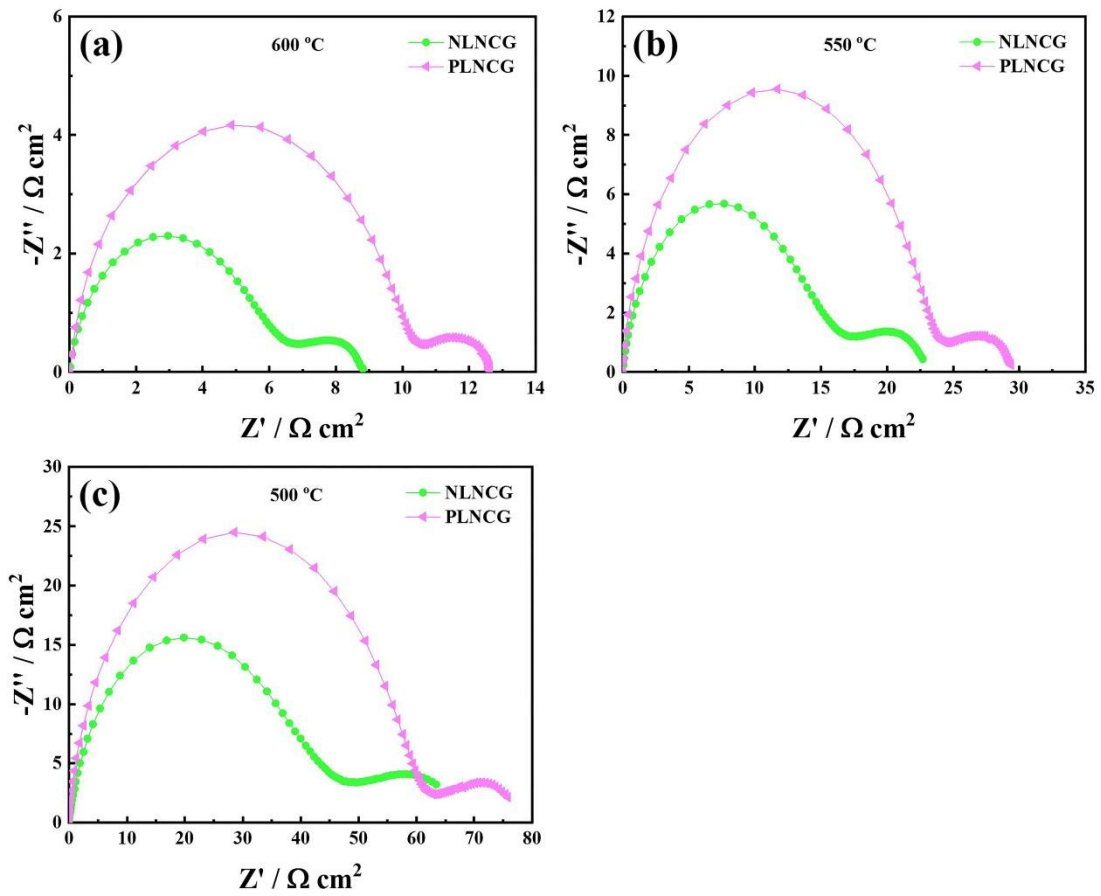


**Fig. S1.** EIS of the symmetrical cell NLNCG|GDC|NLNCG and PLNCG|GDC|PLNCG at (a) 600, (b) 550, and (c) 500 °C, respectively.

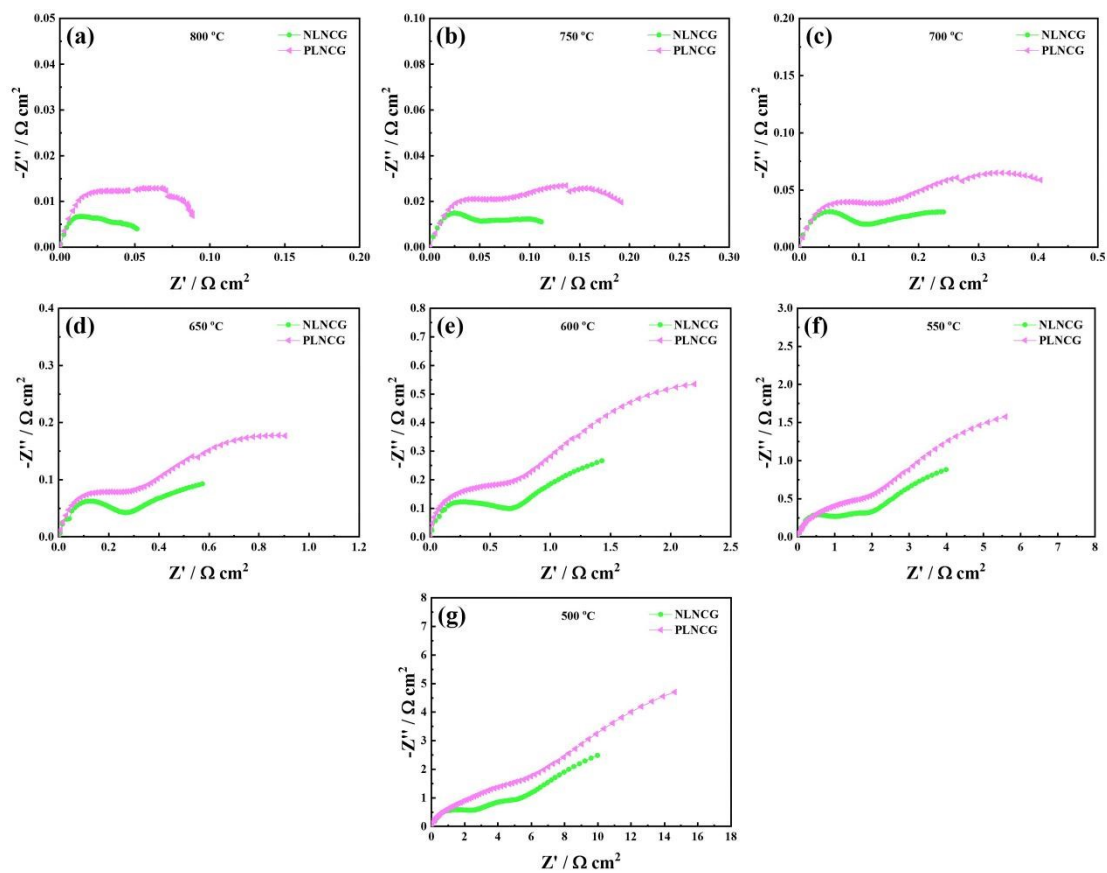


**Fig. S2.** EIS of the symmetrical cell NLNCG|BZCYYb|NLNCG and PLNCG|BZCYYb|PLNCG

at (a) 800, (b) 750, (c) 700, (d) 650, (e) 600, (f) 550 and (g) 500 °C, respectively.

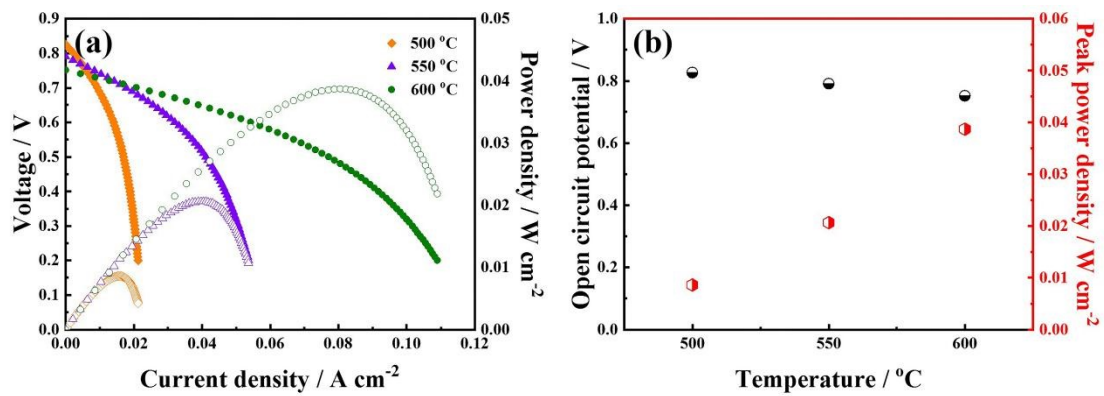


**Fig. S3.** (a) I-V-P curves of the electrolyte supported single cell NiO-GDC|GDC|NLNCG tested at different temperatures, with dry H<sub>2</sub> as fuel and ambient air as oxidant, (b) the derived open circuit potentials and peak power densities.

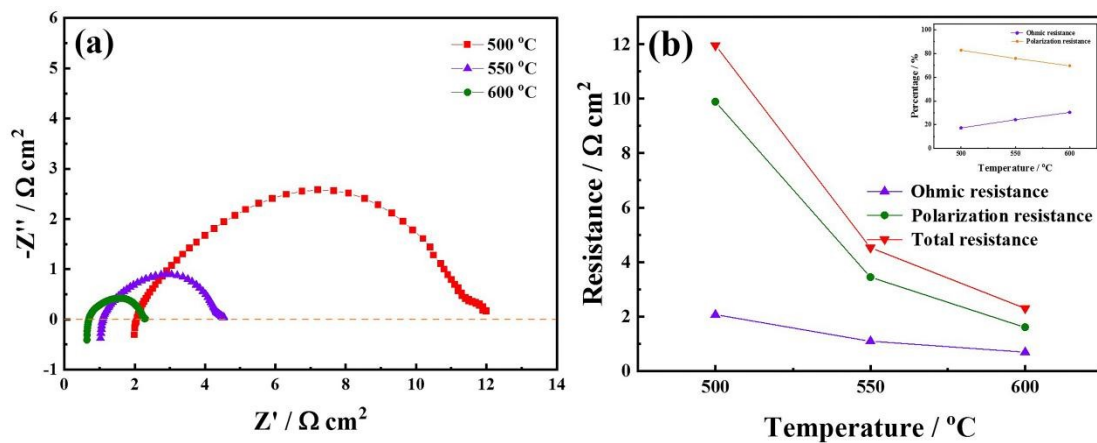


**Fig. S4.** (a) EIS of the electrolyte supported single cell NiO-GDC|GDC|NLNCG measured at open circuit potential, with dry  $\text{H}_2$  as fuel and ambient air as oxidant at different temperatures, (b) the derived ohmic, polarization and total resistances, the illustration in Figure S4b shows the percentages of the ohmic and polarization resistance values compared to that of the total resistance values at different temperatures.